Anomalies of thermoelectric power and of resistance in electronic topological transitions in bismuth and its alloys

N. B. Brandt, V. S. Egorov, M. Yu. Lavrenyuk, N. Ya. Minina, and A. M. Savin

Moscow State University

(Submitted 25 June 1985)
Zh. Eksp. Teor. Fiz. **89**, 2257–2269 (December 1985)

The behavior of the thermoelectric power and resistance of tellurium- and tin-doped single crystals of bismuth and bismuth-antimony alloys were investigated in different electronic topological transitions, of the "Fermi-surface cavity formation (vanishing)" type, induced by anisotropic deformation. For all electronic topological transitions monitored by determining the change of the period of the resistance quantum oscillations in a magnetic field, anomalies were observed in the dependence of the thermoelectric power on the strain. The anomalies took the form of a somewhat smeared asymmetric peak of positive polarity if the electronic topological transition corresponded to the onset of an electron cavity, or of negative polarity in the case of a hole cavity. At $T > 4.2$ K the peak of the thermoelectric power shifted towards greater connectivity of the Fermi surface, and the peak itself became smeared out and vanished in practice at nitrogen temperatures. The resistance variation had a more complicated character in this case.

INTRODUCTION

Much attention is paid in recent studies of electronic topological transitions (ETT) to the anomalies that should be exhibited, according to the familiar paper of I. M. Lifshitz,[1] by the thermodynamic and kinetic characteristics of metals undergoing such transitions. In an analysis[2] of kinetic phenomena near ETT, it was pointed out for the first time that the anomalies of the electric conductivity σ and of the thermoelectric power α are determined primarily by the anomaly of the relaxation time τ. The anomaly of α manifests itself most strongly and takes the form $\alpha \propto |Z|^{-1/2}$, where $Z = E - E_{cr}$ is a transition parameter that characterizes the proximity of the Fermi energy to the critical value E_{cr}. Whereas the form of the anomaly of the conductivity $\sigma = ne^2\tau/m$ is independent of the sign of the charge, the sign of the anomaly of the thermoelectric power $\alpha = (\pi^2 T/3e)\partial \ln\sigma/\partial Z$ is different for electrons and holes, regardless of the initial thermoelectric power of the sample.[1)]

Thermoelectric-power anomalies observed in ETT in lithium-magnesium and cadmium-magnesium alloys as functions of the magnesium-impurity density were already described earlier,[3,4] as was also the anomalous behavior of thermoelectric power in Bi whiskers under tension.[5] Thermoelectric-power anomalies in a two-dimensional electron gas, observed in ETT in a silicon-based MIS structure[6] will change of the gate voltage (and accordingly the electron density) were described in considerable detail quite recently.[6] These results, however, do not account fully for the connection between the thermoelectric peak observed in ETT, on the one hand, and the form of the anomaly of the density of states in the vicinity of the transition, on the other. Nor is account taken of the connection between the carrier relaxation time in real three-dimensional systems and the size of the observed anomaly and its smearing.

The objects used in the present investigation to observe the ETT and the associated anomalies of the thermoelectric power and of the resistance were single crystals of bismuth and of the alloys $Bi_{1-x}Sb_x$ ($x \sim 0.1$), doped with donors and acceptors. The external action that rearranged the energy structure was anisotropic deformation (uniaxial compression, tension, or a combination of the two). This deformation, as noted already in Ref. 1, leads more effectively to the ETT than hydrostatic compression.

The Fermi level of most good metals is as a rule far enough in energy from the critical points E_{cr}, and realization of ETT calls for a rather strong action on the carrier energy spectrum, using factors such as high hydrostatic pressure, doping, or uniaxial deformations. The small overlap energy ($E_{ov} = 43$ meV, Ref. 7) of the fifth and sixth energy bands of bismuth, which determines the metallic properties of the latter, has permitted observation of ETT at relatively low values of the perturbing factors.[5,8,9] As regards to smallness of the characteristic energies of the carrier spectra, bismuth and its alloys are exceedingly convenient objects for ETT observation, since anisotropic deformation easily produces in a single sample of these materials a continuous transition through the critical point E_{cr}. This increases the accuracy of the results, and the very instant of the ETT can be reliably determined from characteristic changes in oscillatory effects. In addition, the action of anisotropic strains on the band structures of these materials has already been investigated in detail earlier,[8] and the deformation potentials were determined in Refs. 10 and 11. All this permits an ETT of a preselected type to be realized in this system, and the transition parameter can be the energy distances to the critical points.

Figure 1 shows schematically the arrangement of the electron and hole extrema of bismuth near the Fermi level (Fig. 1a), and demonstrates the possibility of realizing ETT through doping with donor (Fig. 1b) or acceptor (Figs. 1c and 1d) impurities. Addition of the neutral impurity arsenic influences strongly the relative placement of the L and T extrema,[12] causing inversion of the L_s and L_a terms at an

 0038-5646/85/121303-08$04.00

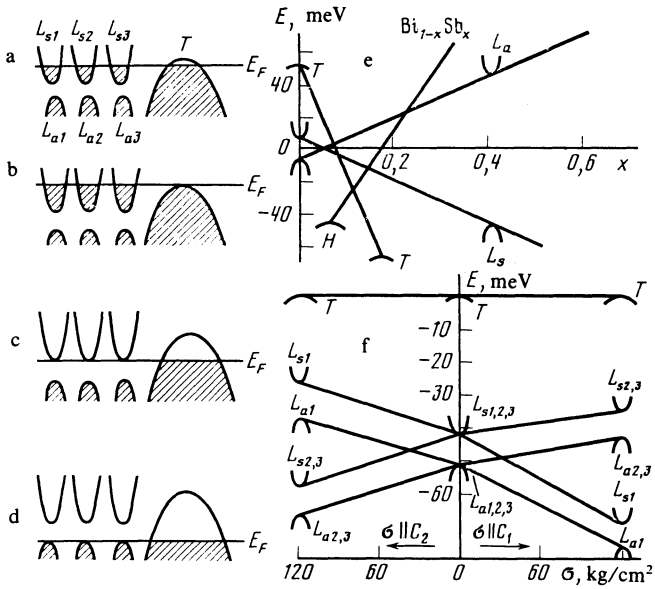

FIG. 1. Schematic arrangement of the electron and hole extrema near the Fermi level of bismuth (a), and rearrangement of the band structure of bismuth by doping with donors (b) and acceptors (c, d), by addition of antimony[12] (e), and by anisotropic deformation[10] (f); in Fig. 13, σ is the stress in compression.

antimony concentration $x = 0.04$, and a transition to the semiconducting state in the concentration interval $0.065 \leqslant x \leqslant 0.22$ (Fig. 1d). The bismuth spectrum is also strongly restructured by anisotropic deformation that upsets the equivalence of the L extrema and leads to redistribution of the carriers among the L_i valleys.[8]

The shift of the L_i extrema relative to the term at the point T for single-crystal bismuth compressed along the binary and bisector axes C_2 and C_1 is illustrated schematically in Fig. 1f. Obviously, a definite choice of the antimony concentration, of the doping with donors and acceptors, and of the magnitude and direction of uniaxial deformation makes it possible to realize in bismuth-antimony alloys electronic topological transitions of the "formation (vanishing) of a new Fermi-surface (FS) cavity" type for any of the extrema shown in Fig. 1a. The uniaxial strains needed for this purpose lie in the realistically attainable region.[8]

We investigate in this paper the anomalies of the thermoelectric power and of the resistance for various ETT accompanied by formation (vanishing) of either electron or hole FS cavities. Preliminary results were published earlier.[13]

EXPERIMENT

To observe ETT with formation (vanishing) of FS electron ellipsoids, we chose the alloys $Bi_{0.9}Sb_{0.1} + 10^{-4}$ at. % Te (type I) and Bu + 10^{-3} at. % Te (type II). A transition with formation of a hole FS at the point T was investigated in samples of Bi + 10^{-2} at. % Sn (type III) and n-$Bi_{0.92}Sb_{0.08}$ (type IV). Samples of type I and II were grown at the Baĭkov Metallurgical Institute, type III at the Moscow State University, and type IV at the Humboldt University (E. Berlin). The control samples without ETT in the investigated strain range were Bi and $Bi_{0.9}Sb_{0.1} + 10^{-3}$ at. % Te.

The samples were cut by the electric-spark method in the form of disks 3 mm in diameter and 0.75 mm thick, with plane parallel to the basal plane of the crystal, and also in the form of rectangular parallelepipeds measuring $3 \times 0.6 \times 0.6$ mm elongated along the C_1 or C_2 axis. The crystals were oriented accurate to $\sim 1°$ along the traces of the secondary slip planes, parallel to C_2, in the basal plane. The antimony concentration was x-ray monitored accurate to 0.3% against the interplanar distances in the [111] direction; the dependence of these distances on the antimony density was determined in Ref. 14. The degree of doping with tellurium and tin was set when the samples were grown. This parameter is tentative, for in final analysis the initial state of the system is determined by the Fermi energy E_F calculated from the experimental FS sections.

The samples were deformed by a procedure described in Ref. 15, by producing a tensile force F in elastic annular yokes (Fig. 2a). In this case, as shown in Ref. 10, the real deformation of a disk-shaped sample is close to uniaxial compression, and the diagonal components of the strain tensor at $F = 30$ kgf, determined by x-ray diffraction, were $\varepsilon_{xx} = 0.13\%$, $\varepsilon_{yy} = -0.3\%$, $\varepsilon_{zz} = 0.1\%$ (the directions of the axes are shown in Fig. 2). The samples were deformed at liquid-helium temperature with a calibrated stretching device, in which a tensile strain along the x axis of an elastic ring was transformed into compression of a sample firmly inserted into this ring along the y axis. A compression strain was produced along the axis C_2 or C_1. We have deformed in the present study, for the first time, parallelepiped samples in an elastic annular yoke (Figs. 2b, c). Large uniaxial compression strains (up to 0.3%) can be obtained in such samples because of the specifics of the plastic flow of bismuth at low temperature, viz., plastic effects evolve primarily by formation of slip planes. Securing the easiest (111) cleavage plane in the ring with "Aral'dit" resin, so that the compressing force is strictly parallel to the ring, makes it possible to increase directly the elastic loading to values at which slip

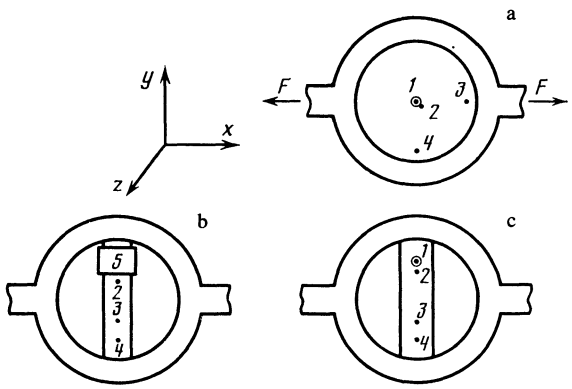

FIG. 2. Arrangement of contacts and heater for the measurement of the thermoelectric power of strained disklike (a) and rectangular (b, c) samples: 1) point-contact heater; 2) "hot" contact; 3, 4,) "cold" contacts; 5) heating coil.

planes begin to evolve in the secondary cleavage planes. The method described can be used to deform all semimetals in the basal plane, and apparently also metals such as zinc and cadmium in the hexagonal plane.

The resistance R of rectangular samples was measured by a standard four-contact method using a V2-34 differential voltmeter, with accuracy not worse than $10^{-6}\Omega$, or was plotted on an $x-y$ recorder. The limitations imposed by the stressing procedure did not permit an exact determination of the absolute value of the thermopower coefficient for long and thin samples by standard methods. We measured the strain dependence of the thermoelectric-power signal produced when a small temperature difference $\Delta T \sim 0.5$ $\varkappa$ ($T = 4.2\varkappa$ and $1.9\ \varkappa$) was produced in the sample. The difference ΔT was produced in a number of cases by heater 5 wound on one of the ends of the sample (Fig. 2b). In the main, however, we used the local heating method frequently employed to measure the thermoelectric power of semiconducting materials. Its advantage is that the investigated region is restricted to the small part of the sample in which the temperature gradient is present. This is also of importance for the investigation of alloys that always contain a certain spatial inhomogeneity.

Local heating at point 1 was produced at the center of round samples (Fig. 2a) or at the edge of rectangular ones (Fig. 2c) by a pointed copper rod of 0.2 mm diameter, on which a $\sim 8\Omega$ heater of manganin wire of 0.05 mm diameter was bifilarly wound. This rod was either pressed to the sample, or soldered to point 1 by Wood's alloy. The "hot" potential contact was located 0.2 mm away from point 1, while the "cold" ones 3 and 4 were near the edge of the disk. The potential contacts were either of beryllium bronze and clamped, or electric-spark welded with copper wires of 0.05 mm diameter, or soldered near the point 1. The measured potential difference $U_{23(4)}$ was the difference between the thermoelectric power of the sample and that of the contact wire, but the main contribution was made by the sample, since measurements have shown that for type-I samples the thermoelectric power at 4.2 K is $\alpha \approx 1 \mu V/\text{K}$, as against $\alpha = 0.15 \mu V/\text{K}$ for beryllium bronze. Nonetheless, especially in the case of soldered contacts, a small background thermoelectric power is present and is due apparently to leakage of some of the heat through the hot contact. This thermopower, as shown by measurements of control samples, has no singularities under stress and does not affect the anomalies described above, but does make a quantitative analysis of their form and relative magnitude difficult. The power released by the heater was chosen to leave contacts 3 and 4 cold, i.e., to have the temperature of the surrounding liquid helium. This was monitored by absence of a U_{34} signal in the presence of a U_{23} signal. The temperature of the hot contact 2 did not change during the stress cycle. The thermoelectric power signal was amplified by an F-116 photoamplifier, was plotted point by point by a null method, or was automatically plotted with an $x-y$ recorder. The circuit was sensitive enough to record a change $\Delta U = 10^{-8}$ V. The dimensions of the FS were monitored during the course of deformation against the quantum oscillations of the resistance or of the thermoelectric power in a magnetic field up to 56 kOe.

The $U_{23(4)}(\varepsilon_{yy})$ and $R(\varepsilon_{yy})$ dependences were investigated in the temperature range 2–100 K. Temperatures higher than 4.2 K were obtained using a foamed-plastic vessel provided with a heater fitted over the device that stretched the annular yoke. In this case the temperature gradient along the sample was monitored with two Cu–CuFe thermocouples, whose copper ends served simultaneously as potential contacts that picked off the thermopower signal.

MEASUREMENT RESULTS

ETT accompanied by appearance (vanishing) of FS electron ellipsoids, of the type "3 electron ellipsoids$\rightleftarrows$1 electron ellipsoid ($3e \rightleftarrows 1e$)," were observed in $Bi_{0.9}Sb_{0.1} + 10^{-4}$ at. % Te single crystals. Doping the semiconducting alloy $Bi_{0.9}Sb_{0.1}$ with donors leads to filling of the electron extrema and to formation of a three-ellipsoid FS with $E_F = (8-10)$ meV. The small Te-density gradient in the ingot from which the samples were cut led to some variation of the initial value of E_F, and to a corresponding shift of the ETT point with respect to strain, but all the regularities observed were common to all 17 type-I samples regardless of the sample shape and of the contact placement.

Compression strain along the C_1 axis causes spillover of all the FS electrons into ellipsoid 1 and vanishing of the remaining ellipsoids 2 and 3 (Fig. 3a). At the transition point $\varepsilon_{yy} = \varepsilon_k = -0.15\%$ the observed cross sections[2)] of the

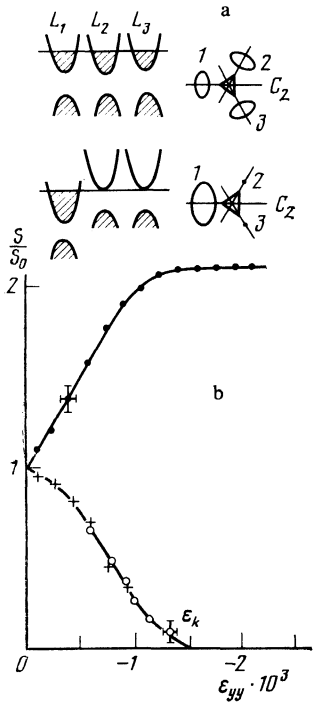

FIG. 3. Electronic topological transition of type $3e \rightleftarrows 1e$ in $Bi_{0.9}Sb_{0.1} + 10^{-4}$ at. % Te samples (sample I-11): a—nonequivalent shift of L terms upon compression along the C_1 axis (perpendicular to C_2), which leads to spillover of the carriers into one extremum; b—relative change of the ellipsoid sections L of sample I-11; ●) increasing ellipsoid, +, ○) decreasing ellipsoids.

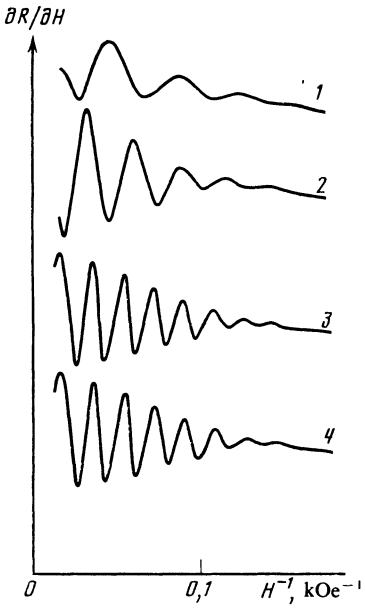

FIG. 4. Growth (curves 1, 2, and 3) and stabilization (4) of the Shubnikov–de Haas oscillations from the L_1 ellipsoid of sample I-11 in a transition of type 3e⇄1e. Strains ε_{yy}: 1 — 0, 2– — 0.07%, 3– — 0.2%, 4– — 0.3%.

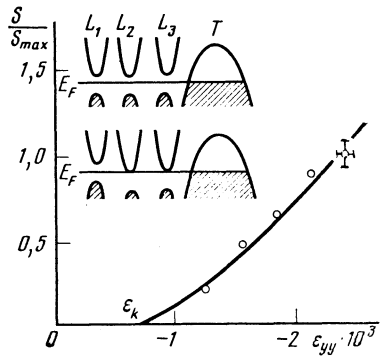

FIG. 6. Growth of electron FS cross sections of Bi + 10^{-2} at. % Sn samples following a transition of the type 1h⇄1h + 2e (Sample II — 1). Solid line—calculation in accordance with the model of Ref. 16. In the upper part of the figure is shown the drop of the terms $L_{2,3}$ below the Fermi level upon compression along C_2, which leads to the appearance of new electron FS.

growing ellipsoid L_1 become stabilized, and those of the decreasing $L_{2,3}$ fall to zero (Fig. 3b). The increase of the cross sections L_1 and their invariance past the ETT point is illustrated in Fig. 4. At the ETT point, the thermopower signal for $\varepsilon_{yy} = \varepsilon_k$ has a maximum, and the resistance increases strongly and goes through a maximum at noticeably higher strains (Fig. 5). In the inset of Fig. 5 the thermopower peak is altered as a function of the transition energy parameter $Z = E - E_{F1}$, where E is the energy distance between the diverging terms L_1 and $L_{2,3}$ and increases with the strain, while E_{F1} is the Fermi energy of the increasing ellipsoid L_1. The divergence of the terms L_1 and $L_{2,3}$ was calculated from the experimental plots of $S(\varepsilon_{yy})$ using the model of the Bi energy spectrum.[16] In its physical meaning, the parameter Z is similar to transition energy parameter introduced by I. M. Lifshitz in Ref. 1; $Z = 0$ at the ETT point. For samples with different initial values of E_F in the underformed state, the ETT point ($Z = 0$) is reached at somewhat different values of ε_k, and the thermopower shift is accordingly shifted.[13]

Formation of two electron ellipsoids at L against the background of the hole ellipsoid at the point T (ETT of 1h⇄1h + 2e type) was observed in Bi + 10^{-2} at. % sam-

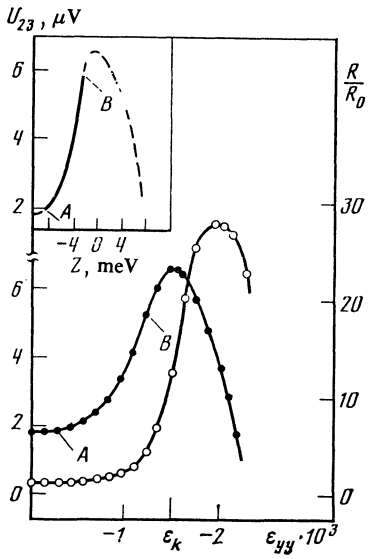

FIG. 5. Anomalies of resistance (right-hand scale, light circles) and thermoelectric power (left-hand scale, dark circles) of stressed sample I-11; ε_k and $Z = 0$ correspond to ETT in accord with oscillation data of Fig. 3b; Z is the energy parameter of the transition; the section AB on the peak of the thermopower is easily extrapolated by the square-root dependence $U_{23} = C_0 + C|Z|^{-1/2}$ (solid line in the inset).

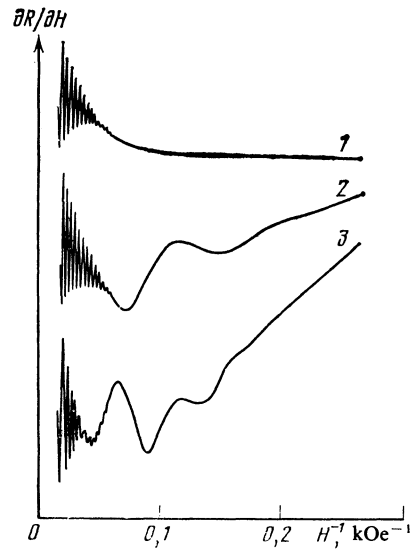

FIG. 7. Onset and growth of frequency of oscillations from the electron ellipsoids $L_{2,3}$ for a 1h⇄1h + 2e transition in sample II-1. Strains ε_{yy}: 1–0; 2– — 0.15%; 3– — 0.24%. The high frequency corresponds to a hole ellipsoid in T.

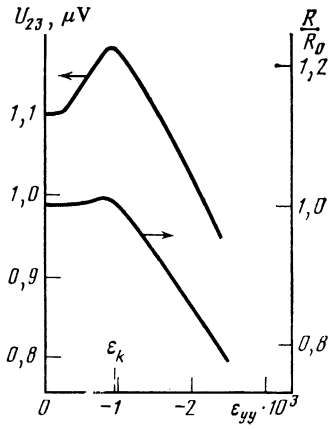

FIG. 8. Anomalies of thermoelectric power (left-hand scale) and of resistance (right-hand scale) of sample II-1 for ETT.

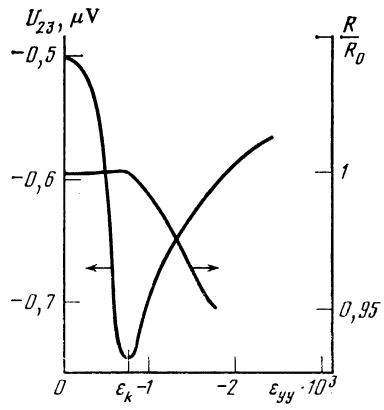

FIG. 10. Anomalies of thermopower (left-hand scale) and resistance (right-hand scale) of Bi + 10^{-3} at. % Te (sample III-2).

ples (Type III) compressed along C_2. The schematic arrangement of the electron and hole extrema and their strain-induced displacement are shown in the upper part of Fig. 6. Owing to the sufficiently strong doping with tin, the initial FS consists only of a hole ellipsoid at the point T [$S_{\min} = 29.5 \cdot 10^{-42}$(g·cm/s)^2], and the Fermi level ($E_{FT} = 49$ meV) lands in the forbidden band (cf. Figs. 1a–1d). In view of the lowering of the terms $L_{2,3}$ upon compression along the C_2 axis, two electron ellipsoids L_2 and L_3 appear at the point T at a certain value $\varepsilon_{yy} = \varepsilon_k$ against the background of the hole ellipsoid. The increase of the cross sections of the ellipsoids L_2 and L_3 with increasing strain is shown in Fig. 6, and the onset of the oscillations associated with them is illustrated in Fig. 7. At the transition point, the thermopower has, as in the case of type-I samples, a peak of positive polarity, and the resistance begins to decrease as a result of the influx of light carriers into $L_{2,3}$ (Fig. 8).

ETT with formation of a hole surface at the point T ($3e \rightleftarrows 3e + 1h$) was effected in Bi + 10^{-3} at. % Te samples (type III). The FS in such an alloys consists of three electron ellipsoids in L, with $E_{FL} = 44$ meV. The distance from the top of the valence band in T to the Fermi level is 2 meV according to the notions concerning the band structure of Bi. The relative divergence of the L_1 and $L_{2,3}$ terms following compression along C_1 was determined from the change of the cross sections S_1 and $S_{2,3}$ of the corresponding electron ellipsoids and amounts to 11 eV per unit strain. The carrier redistribution among the valleys shifts the Fermi level downward relative to the term in T, so that at $\varepsilon_{yy} = \varepsilon_k = -0.1\%$

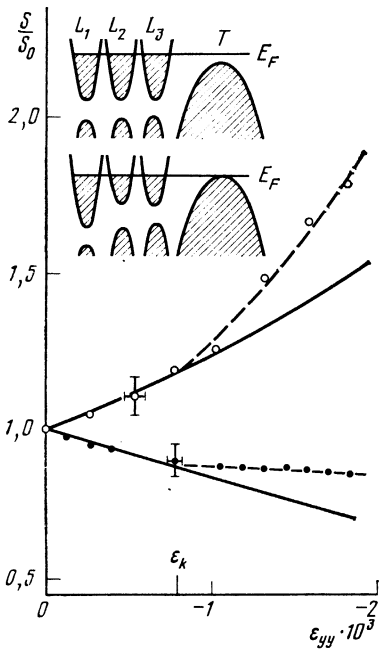

FIG. 9. Relative change of the cross sections of the electron ellipsoids L_1 (○) and $L_{2,3}$ (●) for Bi + 10^{-3} at. % Te (sample III-2) in ETT of type $3e \rightleftarrows 3e + 1h$. Solid lines—calculated according to Ref. 16 in the absence of ETT. In the upper part of the figure is shown schematically the change of the band structure upon compression along C_1, which leads to appearance of a hole ellipsoid in T.

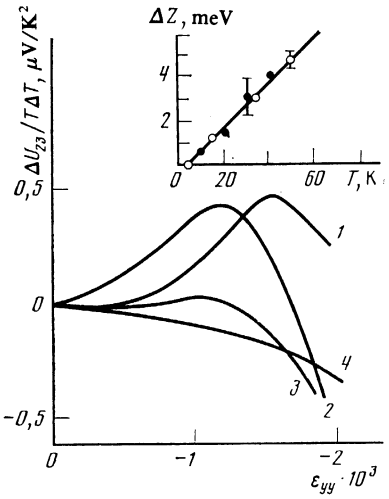

FIG. 11. Shift and broadening of the thermopower peak with rising temperature of sample I-3. Temperature: 1–4.2 K; 2–34 K, 3–52 K, 4–73 K. Inset—plot of the shift of the thermopower peak from its position at $T = 4.2$ K for samples I-3 (○) and I-4 (●) in units of the energy parameter $Z = E - E_{F1}$.

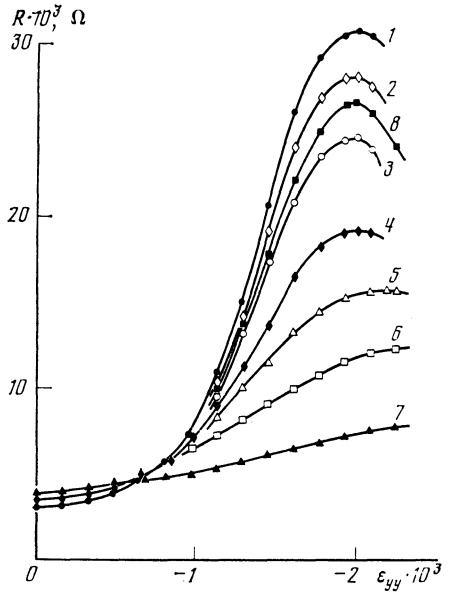

FIG. 12. Resistance peak of sample I-4 at various temperatures: 1–4.2 ж; 2–11 ж; 3–17.5 ж; 4–26 ж; 5–32 ж; 6–41 ж; 7–58.5 ж; 8–14 ж (last deformation cycle).

the Fermi level touches the top of the valence band, and a hole surface appears at point T of the Brillouin zone (see the upper part of Fig. 9 for the term-displacement scheme). Figure 9 shows also the relative changes of the cross sections of the electron ellipsoids L_1 and $L_{2,3}$ for sample III-2 of this series. In the vicinity of ε_k, owing to the overlap with the T-term, the experimental points deviate from the theoretical $S/S_0(\varepsilon_{yy})$ calculated in accordance with McClure's model[16] for the case when no holes are produced in T. The thermopower has at the transition point a peak of negative polarity, and the resistance begins to decrease as a result of the increase of the total number of carriers (Fig. 10).

The semiconductor-semimetal transition already described in Ref. 17 is observed when samples of type IV, of the semiconducting alloy $n-Bi_{0.92}Sb_{0.08}$ with low electron density ($n\sim10^{15}$ cm^{-3}, $E_F\approx1$ meV) due to uncontrollable impurities, are deformed by a compression strain $\varepsilon_{yy}=-0.08\%$ along C_1. At the transition point, the thermopower due to the strain has a clearly pronounced peak of negative polarity, due to the appearance of T-holes, and the resistance drops rapidly because of the overlap of the L and T terms.

Similar measurements were made on a number of control samples of pure Bi and of $Bi_{0.9}Sb_{0.1}+10^{-3}$ at. % Te, in which no ETT takes place in the produced strain region. For all the samples, the investigated dependences of the thermoelectric power and of the resistance on the strain had a smooth character.

The temperature dependence of the observed anomalies in samples of type I was investigated in the interval 2–100 K. Lowering the temperature from 4.2 to 2 K produced no change whatever in the positions and shapes of the thermopower and resistance peaks shown in Fig. 5. Heating to 100 K altered the picture noticeably: the thermopower peak shifted when heated towards lower strains, and its width increased strongly above 30 K and vanished therefore completely at liquid-nitrogen temperature (Fig. 11). For convenience in the comparison of the anomalies recorded at various temperatures and different ΔT, the ordinates in Fig. 11 are the values of $\Delta U_{23}/(T\Delta T)$, where $\Delta U_{23}=U_{23}(\varepsilon_{yy})-U_{23}(0)$. The smearing and shift of the resistance peak with change of temperature are shown in Fig. 12.

DISCUSSION OF RESULTS

It can be stated on the basis of the presented plots of the thermopower and resistance vs strain (see Figs. 5, 8, and 10) that these quantities have anomalies at all types of ETT reliably identified by quantum-oscillation effects. The appearance (vanishing) of an FS cavity is accompanied by an anomaly of the thermopower, in the form of a somewhat smeared and noticeably symmetric peak whose value at 4.2 K is in many cases (e.g., for type-I samples) of the same order of magnitude as the thermopower itself. In qualitative agreement with the theoretical premises,[1,2] the peak is situated within experimental accuracy at the ETT point, and its polarity is determined by the type of carrier of the produced FS cavity, viz., the anomaly is positive for ETT with formation of an electron FS (see Figs. 5 and 8) and negative for a hole FS (see Fig. 10). It should be noted right away that the sign of the thermopower anomaly can serve as a convenient method of identifying the signs of the carriers produced (annihilated) in the course of an ETT.

Great interest attaches to the width and shape of the thermopower peak. It was shown back in 1968 (Ref. 18) that finite damping of electron waves in imperfect crystals smears out the anomalies of the density of states and, accordingly the anomalies expected for ETT in the heat capacity, electron compressibility, and the thermal-expansion coefficient. This smearing permits these effects to be observed in experiment. The differential thermoelectric power in ETT of the type of neck breaking (formation) was very recently calculated.[10] It was found that in the presence of impurities and at finite temperature the thermopower likewise has anomalies, but the peak, which is strongly asymmetric in the pure case, decreases in magnitude and smears out. With rising temperature the peak shifts towards negative Z (towards higher connectivity of the FS) at a rate $\Delta Z=1.28$T.

The shape of the thermoelectric-power peak and its temperature dependence were analyzed for samples of type I. Data on the variation of the FS with strain make it possible to calculate, using the model of Ref. 16, all the characteristic energies in the transition process. Rather than introduce, as earlier in Ref. 13, a transition-energy parameter that varies linearly with the strain ε_{yy}, we use in the present paper the more physical parameter $Z=E-E_{F1}$, equal to the Fermi energy in the rising extrema of $L_{2,3}$ up to the point ε_k, and afterwards to the energy distance from the Fermi level of the carriers spilled over into a single ellipsoid (see Fig. 3a) to the bottom of the $L_{2,3}$ extrema. The quantity Z varies nonlinearly with the strain ε_{yy} up to the point ε_k, and linearly with ε_{yy} beyond that point. In the inset of Fig. 5, the experimental dependence of the thermopower on the strain, shown in the

lower part of the figure, is given in the scale of the parameter Z. In this representation, the anomaly turns out to be more asymmetric, and its shape on the section AB is described by the function $C_0 + C|Z|^{-1/2}$ (solid line in the inset of Fig. 5). The square-root dependence of the anomaly is turned towards negative Z values that correspond, as in Ref. 19, to the region of larger FS connectivity. On the positive side of Z, it is impossible to describe the form of the anomaly analytically with the aid of the asymptotic relations proposed in Ref. 19. The dependence of the thermopower on the strain in that region is determined not only by the considered phase transition, but also by other factors, prominent among which are the overlap with the valence band (see the scheme in Fig. 3a), which should occur according to the calculations of Ref. 10 for type-I samples at $\varepsilon_{yy} = 0.28\%$, and also the still unclear mechanism that determines the change of the resistance at $\varepsilon_{yy} > \varepsilon_k$.

It is reasonable to estimate of the thermopower-peak width in Fig. 5 at the level of the point B, where a square-root descent is observed. Such an estimate yields the value $\Delta Z = 5$ meV (average over five samples), which exceeds substantially the thermal smearing at 4.2 K. After cooling to 2 K, no changes whatever were observed in the anomalies of the thermopower and of the resistance of all the investigated samples. This indicates that the anomaly width at helium temperatures is determined by scattering from impurities.

When the temperature rises, the peak of the thermoelectric power shifts linearly with temperature towards negative values of Z (see Fig. 11), and the shift $\Delta Z = 1.1T$ agrees well with the calculations.[19] Strong smearing of the anomalies begins at temperatures higher than 30 K, when kT becomes comparable with the peak width at $T = 4.2$ K. No thermopower anomaly was observed at liquid-nitrogen temperature. The presence of asymmetry of the thermopower peak (see Fig. 5) and its shift with temperature are evidence that, in the language of Ref. 19, there is realized in the investigated samples a "not very dirty case," when scattering by impurities is comparable with scattering by phonons already at sufficiently low temperature, so that an observable "temperature sensitivity" of the thermopower anomaly takes place. This result correlates well with the data of Ref. 20, in which it is shown that in bismuth-antimony samples of composition close to that of the investigated ones the predominant scattering is by an ionized impurity at liquid-helium temperatures, and by acoustic phonons at $T \gtrsim 10$ K.

Whereas thermopower anomalies are quite distinctly observed for ETT in samples of various types, resistance anomalies are of more complicated and ambiguous character. The reason is that the observed resistance changes are governed mainly by two mechanisms. The first is the change due to the change in the number N of carriers as a result of overlap of the L and T terms at a certain strain value ε_k. This overlap is not observed in the investigated strain region in type-I samples, where N is constant, but determines the resistance drop past the ETT point in samples of type-II (Fig. 8), type-III (Fig. 10), and especially type IV (semiconductor-semimetal transition).

The other mechanism that changes the resistance is due to a transition from isotropic conductivity in the basal plane, when all three L-terms are equivalent, to an anisotropic one when this equivalence is disrupted by the deformation. By the instant when ETT sets in (see Fig. 3a), the sample resistance, initially isotropic in the basal plane, is determined by the anisotropy of the remaining ellipsoid and can in the absence of a hole FS, in accordance with the equations of Ref. 21, either increase by ~ 30 times if it measured in the elongation direction of the remaining ellipsoid, or decrease by one-half if measured in the perpendicular direction. The described mechanism is insignificant in samples III (Fig. 9). In these samples, ETT with formation of a hole FS at the point T takes place against the background of three electron ellipsoids with $E_{FL} \approx 44$ meV, where a slight redistribution of the carriers among the ellipsoids by the instant of the ETT can lead to an increase of the measured resistance by not more than 18%. This holds to equal degree also for type-II samples, where the electron FS is produced against the background of a large hole surface at the point T (see Fig. 6).

The mechanism of the FS anisotropy change becomes decisive in type-I samples. It can explain the increase of the resistance in the direction of the C_1 axis (see Fig. 5) up to $\varepsilon_{yy} = \varepsilon_k$. Subsequently, however, after all the carriers have spilled over into the L_1 extremum, the resistance should not change to the value $\varepsilon_{yy} = -0.28\%$ where, according to the deformation potentials,[10] the hole extrema in L_2 and L_3 rise above the Fermi level and the resistance should decrease because of the increase of the carrier densities. In experiment, however (see Fig. 5), the resistance at $\varepsilon_{yy} > \varepsilon_k$ increases by another factor of two, and then begins to drop at $\varepsilon_{yy} = -0.2\%$. As a result, just as the thermopower, the resistance takes the form of a peak, but one shifted by 5 meV relative to the ETT point. This peak is smeared out with increasing temperature (see Fig. 12), and its position at $T \gtrsim 30$ begins to shift towards larger strains. The position shifted away from the ETT point, and the somewhat different temperature dependence of the peak compared with the thermoelectric power, calls for this anomaly to be of a nature which is difficult to determine at present.

The change of the FS symmetries by deformation should not be substantially manifested in the character of the measured thermoelectric power. The decisive factor here is the possible contribution of the phonon-drag thermoelectric power, which can be anisotropic, in contrast to the diffusion thermopower. The diffusive character of the thermopower at 4.2 K in type-I samples, where the effect of the FS anisotropy change is particularly large, was established in Ref. 22. In addition, as follows from Figs. 5, 8, and 10 of the present paper, the anomaly of the thermopower clearly occurs at the point ε_k for various types of ETT and takes the form of a peak of either polarity regardless of the described mechanisms that determine the behavior of the resistance at the transition point.

The experimental results and their analysis allow us to state that the ETT thermopower anomalies observed in the present study are large and are firmly determined by the state-density anomalies. In the resistance, however, the anomaly of the density of state is weakly manifested, in

agreement with the results of Refs. 2 and 19. Indeed a study[23] of aluminum whisker stretching the observed resistance anomaly did not exceed 0.5%. It is therefore difficult to observe in Bi and in Bi-Sb alloys, against the background of the rapidly varying carrier density and of the FS anisotropy, the resistance anomalies due to the square-root singularity of the density of states at the ETT point.

In conclusion, we take the opportunity to express sincere gratitude to V. G. Vaks, A. V. Trefilov, and A. A. Varlamov for interest in the results and for a helpful discussion.

[1)]We call attention to an error in Ref. 2: the anomaly of the thermoelectric power in the "spillover" case (inset of Fig. 2c) is shown in inverted form.
[2)]According to Ref. 8, all the FS ellipsoid cross sections are altered by the strain in like fashion.

[1]I. M. Lifshitz, Zh. Eksp. Teor. Fiz. **38**, 1569 (1960) [Sov. Phys. JETP **11**, 1130 (1960).
[2]V. G. Vaks, A. V. Trefilov, and S. V. Fomichev, *ibid.* **80**, 1613 (1981) [**53**, 830 (1981)].
[3]V. S. Egorov and A. N. Fedorov, *ibid.* **85**, 1647 (1983) [**58**, 959 (1983)].
[4]V. S. Egorov and S. V. Varyukhin, Pis'ma Zh. Eksp. Teor. Fiz. **39**, 510 (1984) [JETP Lett. **39**, 621 (1984)].
[5]Yu. P. Gaĭdukov, N. P. Danilova, and E. V. Nikiforenko, *ibid.* p. 522 [637].
[6]N. V. Zavaritskiĭ and I. M. Suslov, Zh. Eksp. Teor. Fiz. **87**, 2152 (1984) [Sov. Phys. JETP **60**, 1243 (1984)].
[7]N. B. Brandt, R. Muller, and Ya. G. Ponomarev, *ibid.* **71**, 2268 (1976) [**44**, 1196 (1976)].
[8]N. B. Brandt, V. A. Kul'bachinskiĭ, N. Ya. Minina, and V. D. Shirokikh, *ibid.* **78**, 114 (1980) [**51**, 562 (1980)].
[9]N. B. Brandt and Ya. G. Ponomarev, *ibid.* **55**, 1215 (1968) [**28**, 635 (1969)].
[10]M. Yu. Lavrenyuk, Valence band under strong anisotropic deformations and deformation potentials of bismuth and bismuth–antimony alloys. Abstract of candidate's dissertation, Moscow State Univ., 1984.
[11]K. Walther, Phys. Rev. **174**, 182 (1968).
[12]N. B. Brandt, R. Hermann, G. I. Golysheva, L. I. Devyatkova, D. Kusnik, and Ya G. Ponomarev, Zh. Eksp. Teor. Fiz. **83**, 2152 (1982) [Sov. Phys. JETP 56, 1247 (1982)].
[13]V. S. Egorov, M. Yu. Lavrenyuk, N. Ya. Minina, and A. M. Savin, Pis'ma Zh. Eksp. Teor. Fiz. **40**, 25 (1984) [Tech. Phys. Lett. **40**, 750 (1984)].
[14]M. Berger, B. Christ, and J. Troschke, Crystal Res. and Technol. **7**, 1233 (1982).
[15]N. B. Brandt, V. A. Kul'bachinskii, N. Ya. Minina, and V. D. Shirokikh, Prib. Tekh. Eksp., No. 6, 137 (1979).
[16]J. M. McClure, J. Low Temp. Phys. **25**, 527 (1976).
[17]N. B. Brandt, V. N. Kolosov, V. A. Kul'bachinskiĭ, and N. Ya. Minina, Fiz. Tverd. Tela (Leningrad) **21**, 1971 (1979) [Sov. Phys. Solid State **21**, 1131 (1979)].
[18]M. A. Krivoglaz and Tyu-Hao, Fiz. Met. Metalloved. **21**, 817 (1966).
[19]A. A. Varlamov and A. V. Pantsulaya, Zh. Eksp. Teor. Fiz. **89**, 2188 (1985) [Sov. Phys. JETP **62**, No. 12 (1985)].
[20]N. A. Red'ko, V. N. Pol'shin, V. V. Kosarev, and G. A. Ivanov, Fiz. Tverd. Tela (Leningrad) **25**, 3138 (1983) [Sov. Phys. Solid State **25**, 1807 (1983).
[21]R. N. Zitter. Phys. Rev. **127**, 1471 (1962).
[22]D. R. Overcush, Tracy Davis, J. W. Cook, and M. J. Skove, Phys. Rev. Lett. **46**, 287 (1981).

Translated by J. G. Adashko